



The University of Sydney

School of Civil Engineering
Sydney NSW 2006
AUSTRALIA

<http://www.civil.usyd.edu.au/>

Wind/Environmental Fluids Group

**A New Approximation for Pore Pressure
Accumulation in Marine Sediment due to
Water Waves**

Research Report No R868

**Dong-Sheng Jeng, BE ME PhD
Brian Seymour, BSc, PhD
Jian Li, BSc, MSc, PhD**

April 2006

ISSN 1833-2781



The University of Sydney

School of Civil Engineering
Environmental Fluids/Wind Group
<http://www.civil.usyd.edu.au/>

A New Approximation for Pore Pressure Accumulation in Marine Sediment due to Water Waves

Research Report No R868

Dong-Sheng Jeng, BE ME PhD
Brian Seymour, BSc, PhD
Jian Li, BSc, MSc, PhD

April 2006

Abstract:

The residual mechanism of wave-induced pore water pressure accumulation in marine sediments is re-examined. An analytical approximation is derived using a linear relation for pore pressure generation in cyclic loading, and mistakes in previous solutions (Cheng, et al., 2001, McDougal, et al., 1989) are corrected. A numerical scheme is then employed to solve the case with a non-linear relation for pore pressure generation. Both analytical and numerical solutions are verified with experimental data (Clukey, et al., 1983), and provide a better prediction of pore pressure accumulation than the previous solution (McDougal, et al., 1989). The parametric study concludes that the pore pressure accumulation and use of full non-linear relation of pore pressure become more important under the following conditions: (1) large wave amplitude, (2) longer wave period, (3) shallow water, (4) shallow soil and, (5) softer soils with a low consolidation coefficient.

Keywords:

Pore pressure accumulation, shear stress, cyclic loading, liquefaction

Copyright Notice

Department of Civil Engineering, Research Report R865

A New Approximation for Pore Pressure Accumulation in Marine Sediment due to Water Waves

© 2006 Dong-Sheng Jeng, Brian Seymour and Jian Li

d.jeng@civil.usyd.edu.au Seymour@math.ubc.ca J.li@civil.usyd.edu.au

ISSN 1833-2781

This publication may be redistributed freely in its entirety and in its original form without the consent of the copyright owner.

Use of material contained in this publication in any other published works must be appropriately referenced, and, if necessary, permission sought from the author.

Published by:
School of Civil Engineering
The University of Sydney
Sydney NSW 2006
AUSTRALIA

April 2006

This report and other Research Reports published by The School of Civil Engineering are available on the Internet:

<http://www.civil.usyd.edu.au>

Contents

1. Introduction	4
2. Boundary Value Problem.....	6
3. Source Term	7
3.1 Nonlinear mechanism of pore pressure generation	7
3.2 Linear mechanism of pore pressure generation	8
4. Theoretical Models	9
4.1 Analytical approximation for linear mechanism	9
4.1.1 <i>Finite soil model</i>	9
4.1.2 <i>Shallow soil model</i>	9
4.1.3 <i>Deep soil model</i>	10
4.2 Numerical scheme.....	10
4.3 Comparisons.....	10
5. A Parametric Study	12
5.1 Effects of wave characteristics.....	12
5.2 Effects of soil characteristics	14
6. A Simplified Approximation for an Infinite Seabed	21
6.1 Scaling analysis.....	21
6.2 A simplified approximation for engineering practice.....	21
7. Conclusions	24
Appendix: Mathematical Derivations Of Analytical Solutions.....	24
References	26

1. Introduction[#]

In general, two mechanisms for wave-induced pore pressure have been observed in field measurements and laboratory experiments, as shown in Figure 1. The first results from the transient or oscillatory excess pore pressure and is accompanied by attenuation of the amplitude and phase lag in the pore pressure changes (Madsen, 1978, Yamamoto, *et al.*, 1978). The second mechanism is termed the residual pore pressure, which is the build-up of excess pore pressure caused by contraction of the soil under the action of cyclic loading (Seed and Rahman, 1978, Sumer and Fredsoe, 2002).

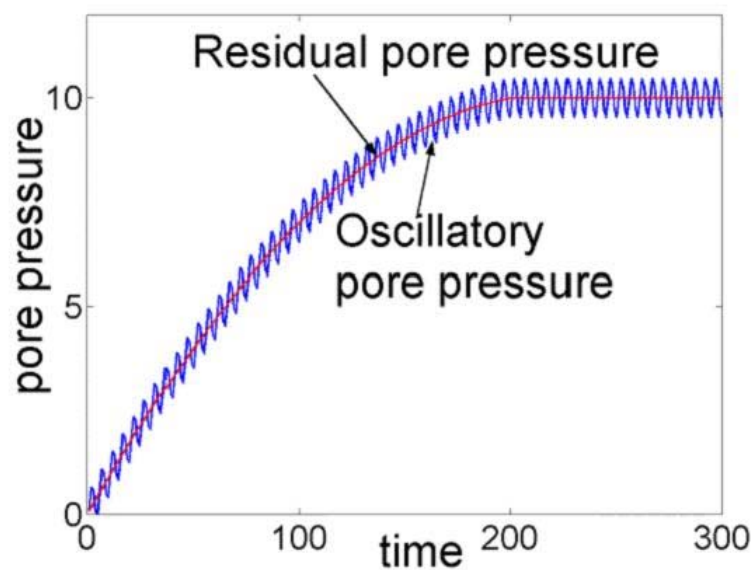


Figure 1: Mechanisms of wave-induced oscillatory and residual pore pressure.

Numerous studies for wave-induced momentary liquefaction, caused by oscillatory pore pressure, were completed in the past few decades. Among these, Yamamoto *et al.* (1978) and Madsen (1978) considered an infinite seabed with a similar framework. Mei and Foda (1981) propose a boundary-layer approximation to derive a rather simplified formulation for the wave-induced transient pore pressure, valid for coarse sand (Hsu and Jeng, 1994). Okusa (1985) further demonstrated the significant influence of the degree of saturation on the pore pressure and proposed the criteria of liquefaction. Jeng (1997) derived a series of analytical solutions for the oscillatory pore pressure within marine sediments. Kianto and Mase (1999) and Yuhi and Ishida (2002) further suggest a new and simplified formulation for the wave-induced pore pressure in a cross-anisotropic seabed.

The mechanism of pore pressure build-up due to ocean waves has also been considered. Seed and Rahman (1978) established a simple one-dimensional finite element model by taking into account the distribution of cyclic shear stresses in the soil profile, and pore-pressure dissipation. Sekiguchi *et al.* (1995) proposed an elasto-plastic model for the standing

[#] Part of this report forms the manuscript: Jeng, D-S, Seymour, B. R. and J. Li (2006): A new approximation for pore pressure accumulation in marine sediment due to water waves. *International Journal for Numerical and Analytical Methods in Geomechanics* (re-submitted, February 2006)

wave-induced liquefaction using a Laplace transformation. Later, some numerical models for post-liquefaction and progressive liquefaction and densification in marine sediments were developed (Miyamoto, *et al.*, 2004, Sassa and Sekiguchi, 1999, Sassa and Sekiguchi, 2001, Sassa, *et al.*, 2001).

In addition to numerical modeling, McDougal *et al.* (1989) proposed a set of analytical solutions for wave-induced pore pressure build-up in a uniform layer of soil, based on the assumption of an incompressible soil. In their approach, the source term in the modified Biot's consolidation equation is derived using a linear relationship between pore pressure ratio (u_g / σ'_o) and cyclic ratio (N / N_ℓ) (Cheng, *et al.*, 2001). To provide a convenient practical result for engineers, McDougal *et al.* (1989) presented their solutions for the cases of shallow, finite and deep soil depths. These analytical solutions are useful for both engineers and researchers, as they can be used for either the investigation of qualitative behaviour of complicated engineering problems or the validation of numerical methods. Recently, using a similar approach, Cheng *et al.* (2001) re-examined the analytical solution of McDougal *et al.* (1989) and proposed a numerical model to investigate the same problem. As pointed out by Cheng *et al.* (2001), the analytical solution proposed by McDougal *et al.* (1989) revealed some errors in the formulations. However, after a close examination of both the McDougal *et al.* (1989) and Cheng *et al.* (2001) solutions, the authors found errors in both publications. Here, we list the original formulae of McDougal *et al.* (1989) and Cheng *et al.* (2001):

Original formulae in McDougal *et al.* (1989) ((28), (33), (36) and (37), pages 6 & 7):

$$F = \frac{d^2 f}{cu_*}, \quad (\text{M-28})$$

$$\frac{\partial U}{\partial T} = \frac{\partial^2 U}{\partial Z^2} + Z[F(Z)]^{-1/\beta^*}, \quad (\text{M-33})$$

$$U(T, Z) = \sum_{n=0}^{\infty} G_n (1 - e^{-K_n^2 t}) \sin(K_n Z), \quad (\text{M-36})$$

$$G_n = \frac{2}{K_n^2} \int_0^1 s [F(s)]^{-1/\beta^*} ds \quad (\text{M-37})$$

Original formulae in Cheng *et al.* (2001) (page 886):

$$\frac{\partial U}{\partial T} = \frac{\partial^2 U}{\partial z^2} + \left(\frac{1+2k_o}{3} \right)^{1+1/\beta^*} Z[F(Z)]^{-1/\beta^*}, \quad (\text{C-33})$$

$$G_n = \left(\frac{1+2k_o}{3} \right)^{1+1/\beta^*} \frac{2}{K_n^2} \int_0^1 s [F(s)]^{-1/\beta^*} \sin(K_n s) ds. \quad (\text{C-37})$$

The correct forms of these equations should read as follows:

$$\frac{\partial U}{\partial T} = \frac{\partial^2 U}{\partial z^2} + Z[F(Z)]^{-1/\beta^*}, \quad (1)$$

$$U(T, Z) = \sum_{n=0}^{\infty} G_n (1 - e^{-K_n^2 T}) \sin(K_n Z), \quad (2)$$

$$G_n = \frac{2}{K_n^2} \int_0^1 s [F(s)]^{-1/\beta^*} \sin(K_n s) ds, \quad (3)$$

$$F(Z) = \frac{d^2}{cu^*} \left[\frac{\tau_{xz}(Z)}{ZP_o \lambda} \right]. \quad (4)$$

The definitions of the symbols used above are the same as those used in the original publications (Cheng, *et al.*, 2001, McDougal, *et al.*, 1989), except β^* representing β in the original paper. As shown above, errors in equation (M-28), (M-36) and (M-37) occurred in the original paper of McDougal *et al.* (1989), while errors of (M-33) and (M-37) occurred in Cheng *et al.* (2001).

All the aforementioned investigations are based on the linear relation of pore pressure generation to cyclic loading proposed in (Seed, *et al.*, 1975, Sumer and Fredsoe, 2002). From previous experiments (De Alba, *et al.*, 1976), this relation is non-linear, rather than linear. However, to the authors' knowledge, to date no analytical solution for the non-linear relations of pore pressure generation is available so numerical methods must be used to get numerical approximation, for example, Seed and Rahman (1978) adopted the finite element method.

In this paper, analytical and numerical techniques for the wave-induced pore water pressure accumulation within marine sediment will be proposed. We derive an analytical solution for the linear relation of pore pressure generation to cyclic loading. Then we investigate the problem with a non-linear relation using a numerical scheme. Both the analytical approximation and numerical model are verified with the previous experimental data. A parametric study then examines the influence of wave and soil characteristics on the pore pressure accumulation in a marine sediment. The effect of a non-linear relation on pore pressure generation is also examined.

2. Boundary Value Problem

For the problem of wave-seabed interaction, the Biot consolidation equations (Biot, 1941) have been generally adopted to model the dynamic response of marine sediments for various applications. In general, the wave-induced pore pressure within marine sediments consists of two components: oscillatory (\tilde{p}) and residual (u) mechanisms, which can be expressed as

$$p = \tilde{p} + u, \quad (5)$$

where p is the pore water pressure, \tilde{p} represents the oscillatory pore pressure that leads to momentary liquefaction, while u represents the period-averaged pore pressure that leads to residual liquefaction, and is defined by

$$u = \frac{1}{T} \int_t^{t+T} p dt, \quad (6)$$

where T is the wave period and t is the time.

A series of analytical solutions for the oscillatory pore pressure within marine sediments have been developed since the 1970's (Jeng, 1997, Jeng and Hsu, 1996, Madsen, 1978, Yamamoto, *et al.*, 1978). The amplitude of the oscillatory pore pressure (\tilde{p}_o) and shear stress (τ_o) for a saturated seabed are given for a seabed of finite thickness by:

$$\tilde{p}_o = \frac{P_b}{1-2\mu} \left[(1-2\mu)(C_2 e^{-kz} - C_4 e^{kz}) + (1-\mu)(\delta^2 - k^2)(C_5 e^{-\delta z} - C_6 e^{\delta z}) \right], \quad (7)$$

$$\tau_o = P_b \left[(C_1 - C_2 kz) e^{-kz} - (C_3 - C_4 kz) e^{kz} + k\delta(C_5 e^{-\delta z} - C_6 e^{\delta z}) \right], \quad (8)$$

where $P_b = \gamma_w H / 2 \cosh kd$ is the amplitude of dynamic wave pressure, μ is the Poisson's ratio, k is the wave number and the C_i ($i=1, \dots, 6$) coefficients and the parameter δ can be found in (Jeng and Hsu, 1996).

For an infinite seabed,

$$p_\infty = P_b e^{-kz} \text{ and } \tau_\infty = P_b k z e^{-kz}. \quad (9)$$

As shown in ((9)), the wave-induced pore pressure and shear stress in an infinite seabed are independent of soil characteristic and are identical to the solution for an incompressible soil and pore fluid (McDougal, *et al.*, 1989). However, (7) and (8) are more general than the solution derived from Laplace's equations (McDougal, *et al.*, 1989).

The residual pore pressure (u) in a homogenous, isotropic soil can be derived from the one-dimensional Biot's consolidation equation (Sumer and Fredsoe, 2002)

$$\frac{\partial u}{\partial t} = c_v \frac{\partial^2 u}{\partial z^2} + f, \quad (10)$$

where f is the mean accumulation pore pressure source term associated with the surface water waves (McDougal, *et al.*, 1989). A detailed derivation of (10) can be found in (Sumer and Fredsoe, 2002). In (10), c_v is the coefficient of consolidation, given by

$$c_v = \frac{2Gk_z(1-\mu)}{\gamma_w(1-2\mu)}. \quad (11)$$

To solve (10), the following boundary and initial conditions are required:

$$u(z,0) = u(0,t) = 0, \quad (12)$$

$$\frac{\partial u(h,t)}{\partial z} = 0 \text{ or } u(\infty,t) = 0. \quad (13)$$

3. Source Term

We now investigate the “*source term*” of the pore pressure generation (f), and consider both linear and nonlinear mechanisms of pore pressure generation.

3.1 Nonlinear mechanism of pore pressure generation

The laboratory results of De Alba *et al.* (1976) relate the development of pore water pressure to the number of load cycles in simple shear. Their non-linear relationship is given by

$$\frac{u_g}{\sigma'_0} = \frac{1}{2} + \frac{1}{\pi} \sin^{-1} \left[2 \left(\frac{N}{N_l} \right)^{1/\theta} - 1 \right], \quad (14)$$

or

$$\sin\left(\frac{\pi u_g}{2\sigma'_o}\right) = \left(\frac{N}{N_\ell}\right)^{\frac{1}{2\theta}}, \quad (15)$$

where u_g is the pore pressure generation due to cyclic loading, σ'_o is the effective overburden, N is the number of cyclic loading, N_ℓ is the number of cycles to liquefaction, and θ is the shape factor suggested to be 0.7 (Seed, *et al.*, 1975).

The pore pressure source term in (10) is given by Seed *et al.* (1975) as

$$f = \frac{\partial}{\partial t} \left(\sigma'_o \frac{N}{N_\ell} \right). \quad (16)$$

3.2 Linear mechanism of pore pressure generation

To simplify the problem, a linear mechanism of pore pressure generation was proposed (Seed, *et al.*, 1975, Sumer and Fredsoe, 2002)

$$\frac{u_g}{\sigma'_o} = \frac{N}{N_\ell}, \quad (17)$$

from which the source term of pore pressure generation can be expressed as

$$f = \frac{\partial}{\partial t} \left(\sigma'_o \frac{N}{N_\ell} \right) = \frac{\partial}{\partial t} \left(\sigma'_o \frac{t/T}{N_\ell} \right) = \frac{\sigma'_o}{TN_\ell}, \quad (18)$$

where T is the wave period and N is the number of cyclic loading periods. In (18), N_ℓ is the number of cycles to liquefaction, which is a function of the cyclic shear stress ratio (Seed and Rahman, 1978, Sumer and Fredsoe, 2002),

$$N_\ell = \left[\frac{\tau}{\alpha\sigma'_o} \right]^{-1/\beta}, \quad (19)$$

where τ is the amplitude of wave-induced shear stress, and λ and β are the functions of the soil type and relative density.

Substituting (19) into (18), we have

$$f = \frac{\sigma'_o}{T} \left[\frac{\tau}{\alpha\sigma'_o} \right]^{1/\beta} \quad (20)$$

which is a generalised definition of the source term.

It is noted that the linear mechanism of pore pressure generation was first applied to the wave-induced pore pressure build-up in marine sediment by Seed and Rahman (1978). Since then, this relation has been commonly used in various approaches (Cheng, *et al.*, 2001, McDougal, *et al.*, 1989, Seed and Rahman, 1978). We will consider the full non-linear relation of pore pressure generation and examine its influence.

4. Theoretical Models

4.1 Analytical approximation for linear mechanism

The shear stress in the source term depends on both wave and soil characteristics. Since the expression for the shear stress in a seabed of finite thickness, i.e., equation (8), is complicated, similar to McDougal et al. (1989), we consider two simplified cases, shallow soil depth and deep depth in addition to the finite soil model. We only outlined the analytical solutions in this section, as detailed derivations are available in Appendix.

4.1.1 Finite soil model

For the finite soil depth, the complete function, (17) is required for the source term. Using a Fourier series expansion, the residual pore pressure can be expressed as

$$u = \sum_{n=1}^{\infty} a_n \left(1 - e^{-c_v \kappa_n^2 t / h^2}\right) \sin\left(\frac{\kappa_n z}{h}\right) \quad (21)$$

$$a_n = \frac{2h}{c_v \kappa_n^2} \int_0^h f(r) \sin\left(\frac{\kappa_n r}{h}\right) dr \quad (22)$$

where f is given in (20), and $k_n = \frac{(2n-1)\pi}{2}$.

4.1.2 Shallow soil model

For relatively shallow soil depth, $h/L < 0.1$, we consider the shallow depth approximation, in which the shear stress can be expressed as

$$\tau = m P_b z, \quad (23)$$

where the value of m can be determined by equating (8) and (23), and integrated over the entire soil depth, yielding

$$m = \frac{2}{kh^2} \left\{ -(C_1 e^{-kh} + C_3 e^{kh}) + (C_2 e^{-kh} - C_4 e^{kh}) + C_1 - C_2 + C_3 + C_4 \right. \\ \left. + kh(C_2 e^{-kh} + C_4 e^{kh}) - k^2(C_5 e^{-\delta h} + C_6 e^{\delta h}) + k^2(C_5 + C_6) \right\}. \quad (24)$$

Then, the source term for shallow soil depth can be further simplified as

$$f = az, \quad (25)$$

$$a = \frac{(1+2K_o)\gamma'}{3T} \left[\frac{3mP_b}{\alpha(1+2K_o)\gamma'} \right]^{1/\beta}, \quad (26)$$

The residual pore pressure can again be given by a Fourier series as

$$u = \frac{a}{2c_v} \left[\left(h^2 z - \frac{z^3}{3} \right) - \sum_{n=1}^{\infty} a_n e^{-c_v \kappa_n^2 t / h^2} \sin\left(\frac{\kappa_n z}{h}\right) \right], \quad (27)$$

$$a_n = \frac{2}{h} \int_0^h \left(h^2 r - \frac{r^3}{3} \right) \sin\left(\frac{\kappa_n r}{h}\right) dr \quad (28)$$

4.1.3 Deep soil model

For soil depth in the range $h/L > 0.3$, we consider the deep (infinite) depth approximation, in which the shear stress is given by (9). The source term for deep soil can be expressed as

$$f = bz e^{-\lambda z}, \quad (29)$$

$$\lambda = \frac{k}{\beta} \quad \text{and} \quad b = a \left(\frac{k}{m} \right)^{1/\beta}. \quad (30)$$

Then, the residual pore pressure is calculated using a Laplace transformation as

$$u = \frac{2b}{c_v \lambda^3} \left[1 - \left(\frac{\lambda z}{2} + 1 \right) e^{-\lambda z} - \frac{1}{\pi} \int_0^{\infty} \frac{e^{-rc_v \lambda^2 t}}{r(1+r)^2} \sin(\sqrt{r} \lambda z) dr \right]. \quad (31)$$

The solution (31) is similar to the one proposed by McDougal et al. (1989) with corrections pointed out previously. It is noted that the shear stress used in the McDougal et al. (1989) solution was based on the assumption of an incompressible soil.

4.2 Numerical scheme

Equation (6) and the Neumann boundary condition are discretised by the following second-order accuracy formulations

$$\begin{aligned} \frac{u(z, t + \Delta t) - u(z, t)}{\Delta t} = \frac{1}{2} c_v \left[\frac{u(z + \Delta z, t + \Delta t) - 2u(z, t + \Delta t) + u(z - \Delta z, t + \Delta t)}{\Delta z^2} \right. \\ \left. + \frac{u(z + \Delta z, t) - 2u(z, t) + u(z - \Delta z, t)}{\Delta z^2} \right] + \frac{1}{2} [f(z, t + \Delta t) + f(z, t)] \end{aligned} \quad (32)$$

and

$$\frac{3u(h, t + \Delta t) - 4u(h - \Delta z, t + \Delta t) + u(h - 2\Delta z, t + \Delta t)}{2\Delta z} = 0. \quad (33)$$

It is easy and fast to numerically solve equations (32) and (33) with the initial and boundary conditions (12) and (13), if we algebraically deal with last two equations to rewrite the system as a tri-diagonal system. In our computations, we use a time transformation so that we can use a small time step size and finite computational times to obtain the numerical solution for large times.

4.3 Comparisons

Here the experimental data of Clukey et al. (1983) is compared with the present solutions. Several tests were conducted in a small wave tank (Clukey, *et al.*, 1983), and numerous sets of wave-induced liquefaction observations were presented in their report. A comparison of the calculated and measure pore pressure accumulation for the two soils is shown in Figure 2. The input data of the experiments (Clukey, *et al.*, 1983) and the numerical calculations are tabulated in Table 1. The results of the previous analytical solutions (McDougal, *et al.*, 1989) (dashed lines), the present linear approximation (solid lines) and nonlinear numerical solutions (solid lines with symbols) are included in the comparison. The relative soil depth for the data is in the range of $0.2 < h/L < 0.3$, hence the soil depth is intermediate. As shown in the figure, the present solutions (both analytical and numerical) are approaching to the experimental data, and provide a slightly better prediction than that of McDougal (1989).

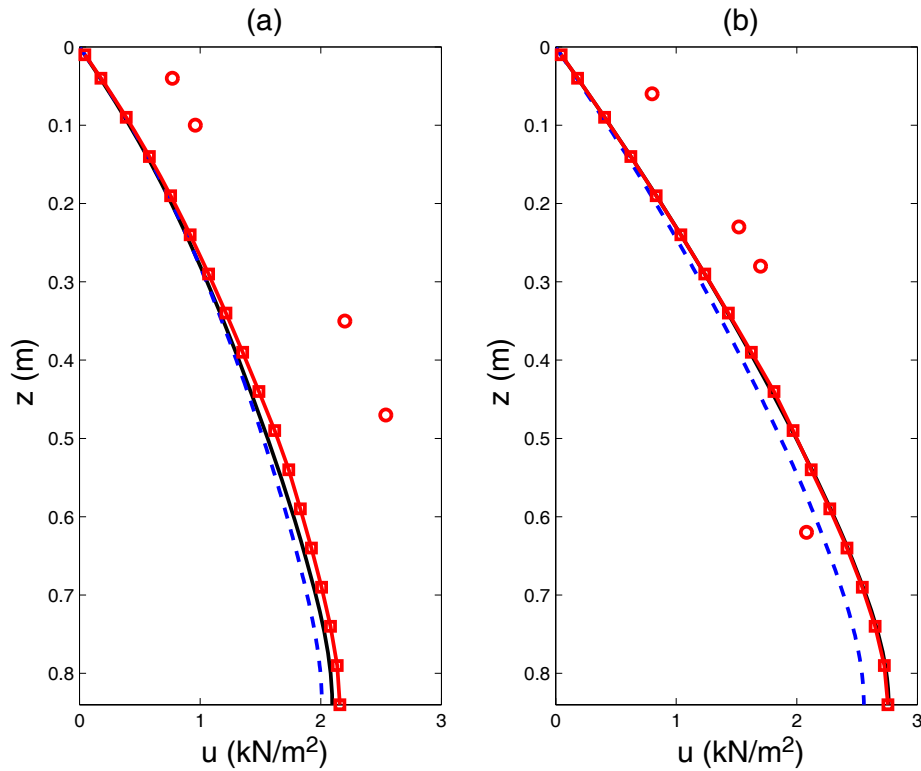


Figure 2: Comparison of the previous model (McDougal, *et al.*, 1989), present analytical and numerical models and experimental data (Clukey, *et al.*, 1983). Notations: (-----) the previous model (McDougal, *et al.*, 1989), (—) the present analytical solution, (—□—) the present numerical model, and (o) experimental data

Table 1: Input data of experiments (Clukey, *et al.*, 1983)

Wave characteristics			Soil characteristics	
	(a)	(b)		
Wave period (T)	1.76 sec	2.02 sec	seabed thickness (h)	0.84 m
Water depth (d)	0.5 m	0.5m	Poisson's ratio (μ)	0.49
Wave length (L)	3.473m	4.103m	Soil porosity (n_e)	0.46
Wave height (H)	0.22 m	0.21m	Shear modulus (G)	5.6×10^5 N/m ²
			Soil permeability (K)	4×10^{-8} m/sec
			Unit weight of soil (γ_s)	$1.8668 \gamma_w$
			Unit weight of pore fluid (γ_w)	9806 N/m ³
			Degree of saturation (S)	1
			Coefficient of earth pressure (Yamamoto, <i>et al.</i>)	0.4
			Consolidation coefficient (c_v)	0.0001165
			α	0.246
			β	0.165

5. A Parametric Study

The primary objective of this paper is to investigate the effects of the non-linear relation of pore pressure generation relation on the wave-induced pore water pressure accumulation in marine sediments. In this section, a parametric study is carried out to examine the influence of five important parameters: wave height, wave period, water depth, seabed thickness and soil type. The input data for the parametric study is given in Table 2.

Table 2: Input data for numerical examples

Soil characteristics	Soil A	Soil B
Poisson's ratio (μ)	0.35	0.49
Soil porosity (n_e)	0.3	0.46
Shear modulus (G)	5×10^6 N/m ²	10^6 N/m ²
Soil permeability (K)	10^{-6} m/sec	10^{-7} m/sec
Unit weight of soil (γ_s)	$2.65 \gamma_w$	$2.65 \gamma_w$
Unit weight of pore fluid (γ_w)	9806 N/m ³	9806 N/m ³
Degree of saturation (S)	1	1
Coefficient of earth pressure	0.5	0.5
Consolidation coefficient (c_v)	0.00221	0.00052
α	0.246	0.246
β	0.165	0.165

5.1 Effects of wave characteristics

Wave height is one important wave characteristics in the design of coastal structures, as it directly affects the wave forces, pressure and energy acting on the structures. It also significantly affects the wave-induced pore pressure and effective stresses in marine sediments (Jeng, 1997). Here we consider the case of non-breaking waves, in which the maximum wave steepness satisfies:

$$(H/L)_{\max} \leq 0.142 \tanh\left(\frac{2\pi d}{L}\right) \text{ and } \left(\frac{H}{d}\right) \leq 0.78. \quad (34)$$

Figure 3 illustrates the distribution of pore pressure accumulation (u/σ'_0) versus time (t/T) for two different soils for three values of H/L . In the figure, solid lines represent the results using the non-linear relation (numerical model) and dashed lines denote the traditional linear relation (analytical approximation). As shown in Figure 3, the pore pressure accumulates faster under large wave loading (Figure 3(b) & (c)), while it will take longer to build-up with small waves (Figure 3(a)). Also, the influence of non-linear relations on the pore pressure accumulation becomes more important as wave steepness increases, comparing Figure 3(a)-(c). It is noted that the line at $\frac{u}{\sigma'_0} = 1$ is the criterion of residual liquefaction.

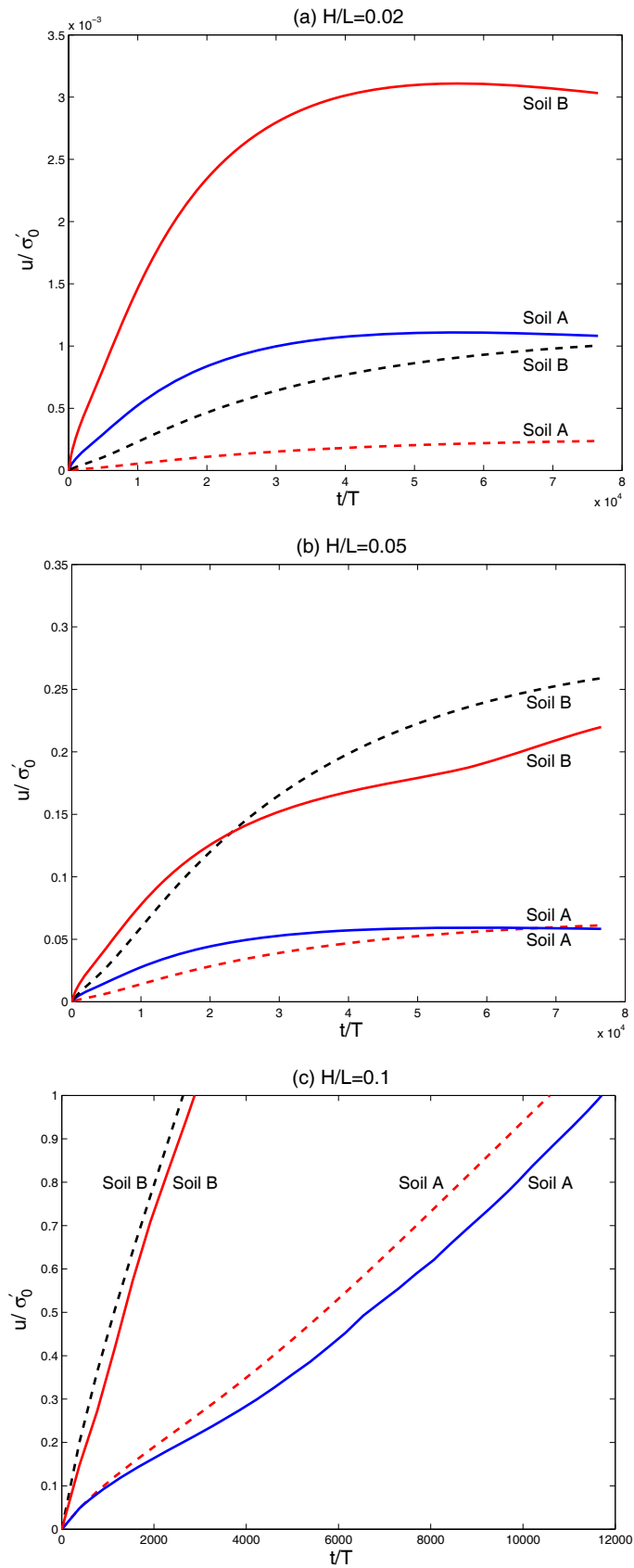


Figure 3: Time development of the pore pressure at $z=2\text{m}$, (---) linear relation, (—) non-linear relation. ($T=10$ sec, $d=16$ m, $h=20$ m)

Wave period and water depth are two parameters that are used to determine the wavelength. In general the wave period varies from 5 sec. to 15 sec. for ocean waves. The pore pressure accumulations for three wave periods are plotted in Figure 4. The figure clearly indicates that the pore pressure builds up faster for short period waves because the pore pressure and energy are more difficult to drain out in a short duration. However, the accumulated pore pressure increases as wave period increases because the higher wave energy can accumulate in a long period wave. It is noted that the results presented in Figure 4 are based on the same wave height for various wave periods. For a short period wave, such as $T=5$ sec, the pore pressure can be built up quickly and become larger under large wave loading.

The relative water depth (d/L) is an index to classify the wave field. For example, we consider water to be shallow if $d/L \leq 0.05$, and deep if $d/L \geq 0.5$, and intermediate water between them. The effect of relative water depth on the pore pressure accumulation is illustrated in Figure 5. The results clearly indicate that the accumulated pore pressure is larger in shallow water than that in deep water, and that the effect of using the nonlinear relation is more significant in shallow water. Note that the vertical scales in the sub-figures in Figure 5 are different.

Based on the results presented in Figures 3-5, it can be concluded that the mechanism of pore pressure build-up and the nonlinear relation for pore pressure generation are more important under the conditions of: (1) larger amplitude waves, (2) longer wave periods, and (3) shallow water.

5.2 Effects of soil characteristics

Besides wave characteristics, soil properties are also important for the wave-induced pore pressure in marine sediment (Jeng, 1997). In this section, we examine two important soil parameters, seabed thickness and soil types.

Figure 6 illustrates the effects of seabed thickness on the pore pressure accumulation in marine sediments. Here the pore pressure can build up faster and accumulate to a large value in shallow soil (Figure 6(a)). The numerical solution for the soil B in Figure 6(a) shows the singularity which is caused by a singular point at some t in the source term with the nonlinear relation.

Referring to Figures 2-6, two different soils are considered in the examples. Soil B with a low consolidation coefficient ($c_v = 0.0052$) can accumulate the pore pressure to a large value, which implies that residual liquefaction is more likely to occur.

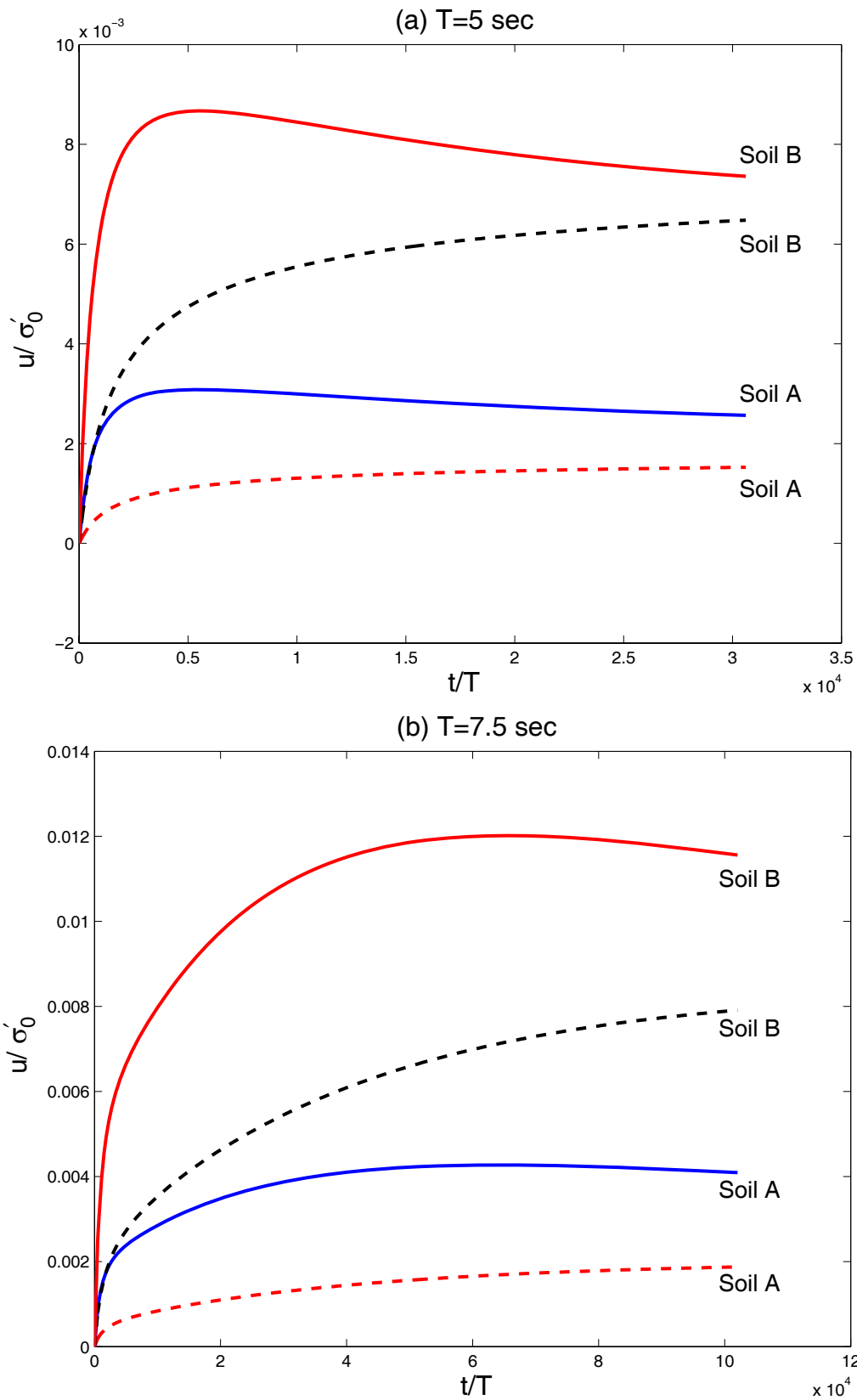


Figure 4(a)-(b): Time development of the pore pressure at $z=2m$, (---) linear relation, (—) non-linear relation. ($H=4$ m, $d=16$ m, $h=20$ m) (a) $T=5$ sec and (b) $T=7.5$ sec.

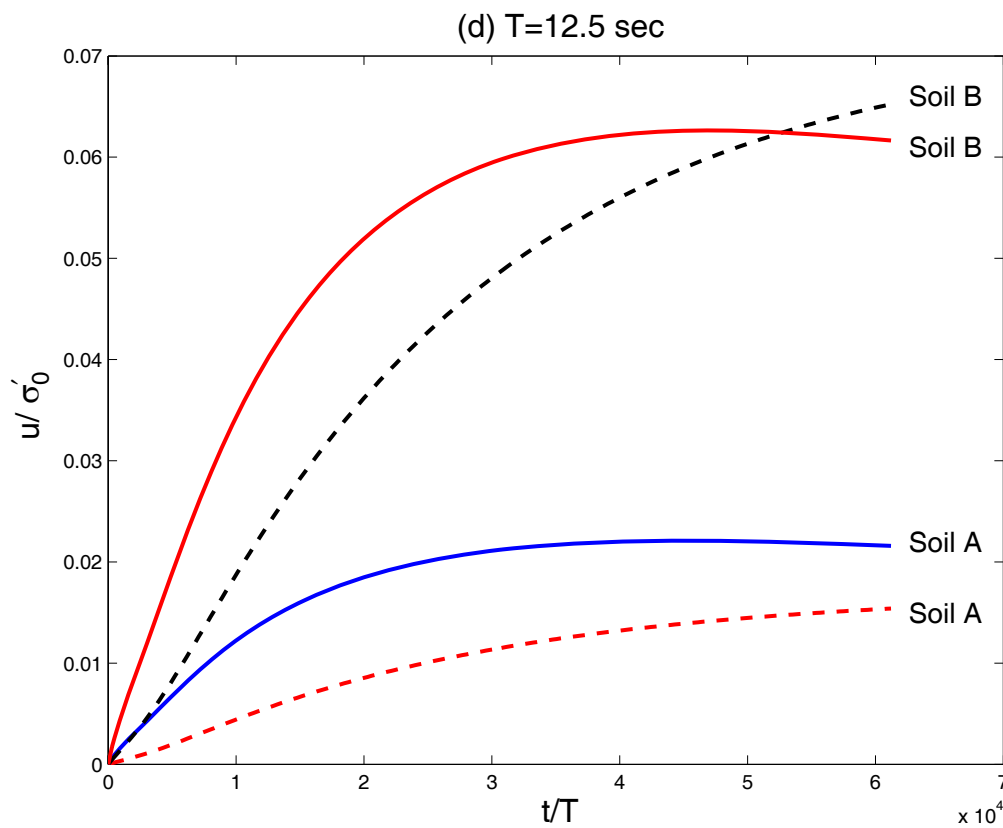
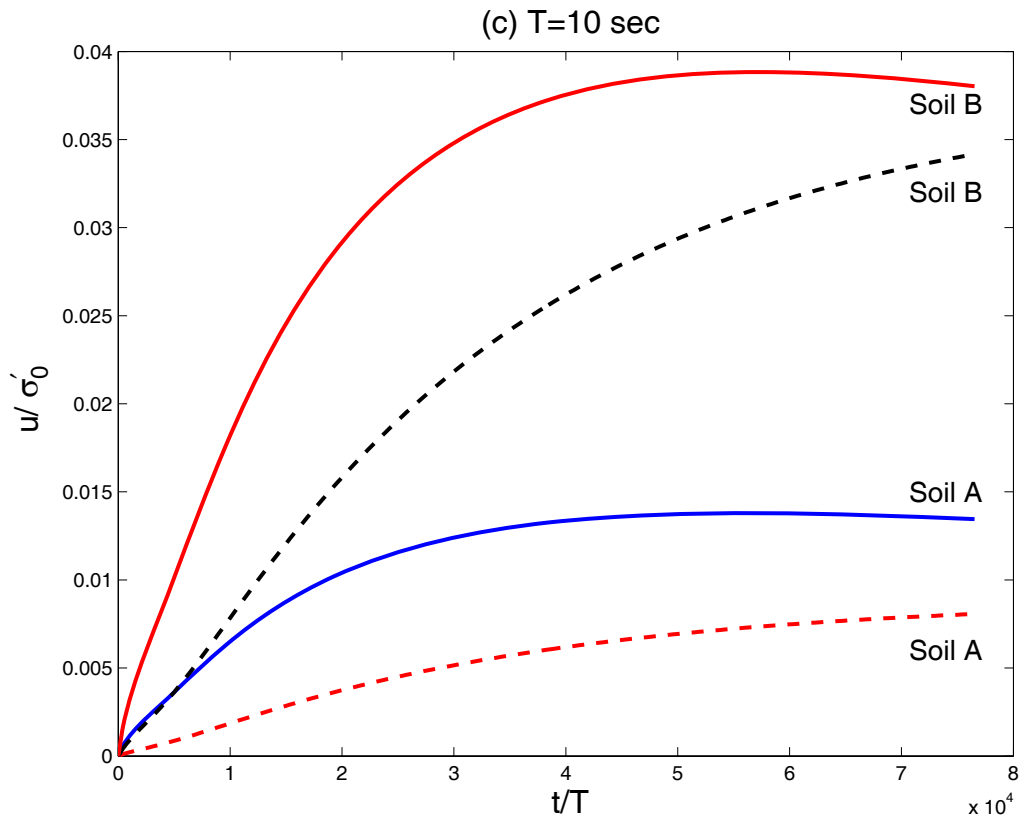


Figure 4(c)-(d): Time development of the pore pressure at $z=2m$, (---) linear relation, (—) non-linear relation. (H=4 m, d=16 m, h=20 m) (a) T=10 sec and (b) T=12.5 sec.

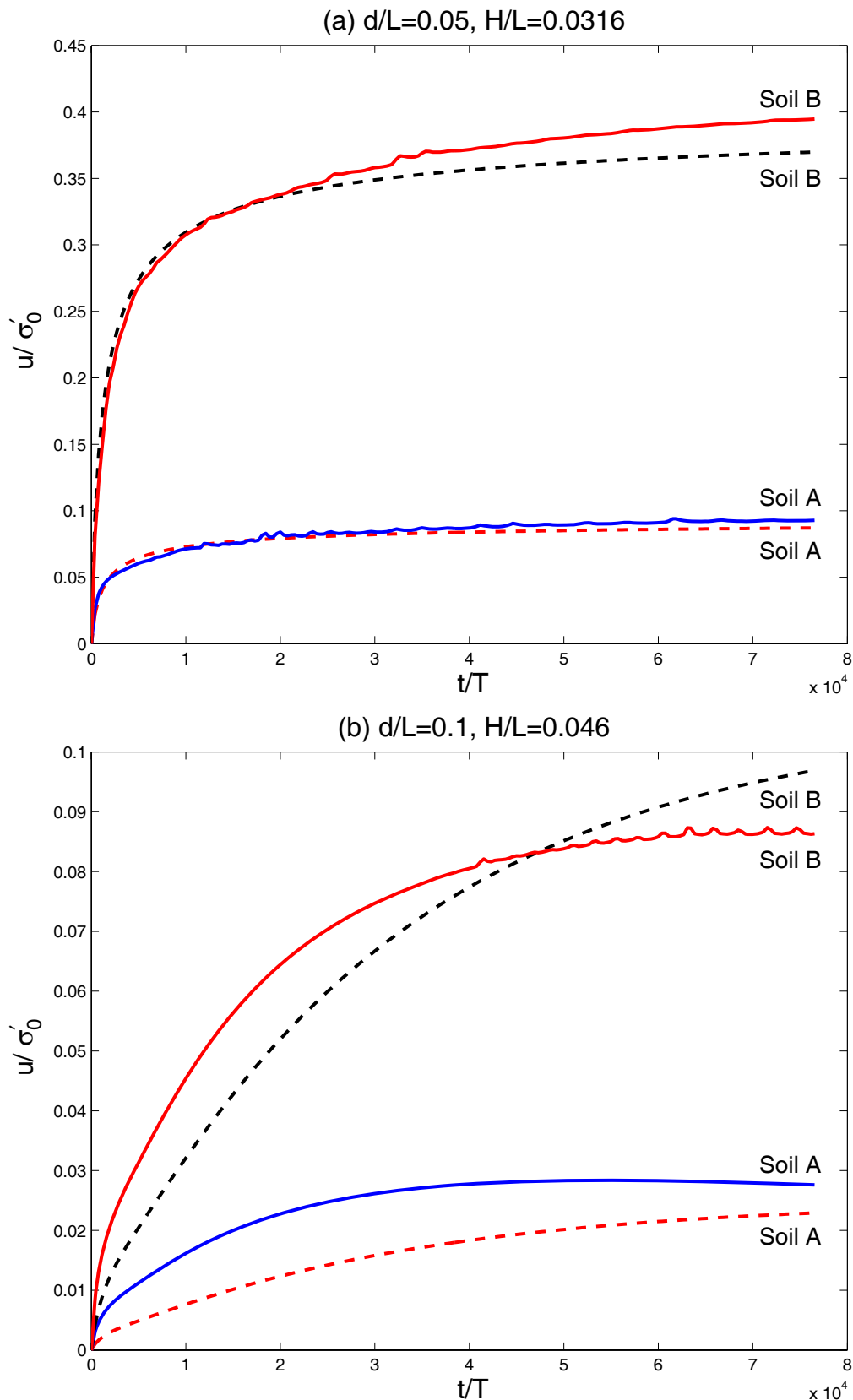


Figure 5 (a)-(b): Time development of the pore pressure at $z=2\text{m}$, (---) linear relation, (—) non-linear relation. ($T=10$ sec, $h=20$ m). (a) $d/L=0.05$, $H/L=0.0316$; (b) $d/L=0.1$, $H/L=0.046$.

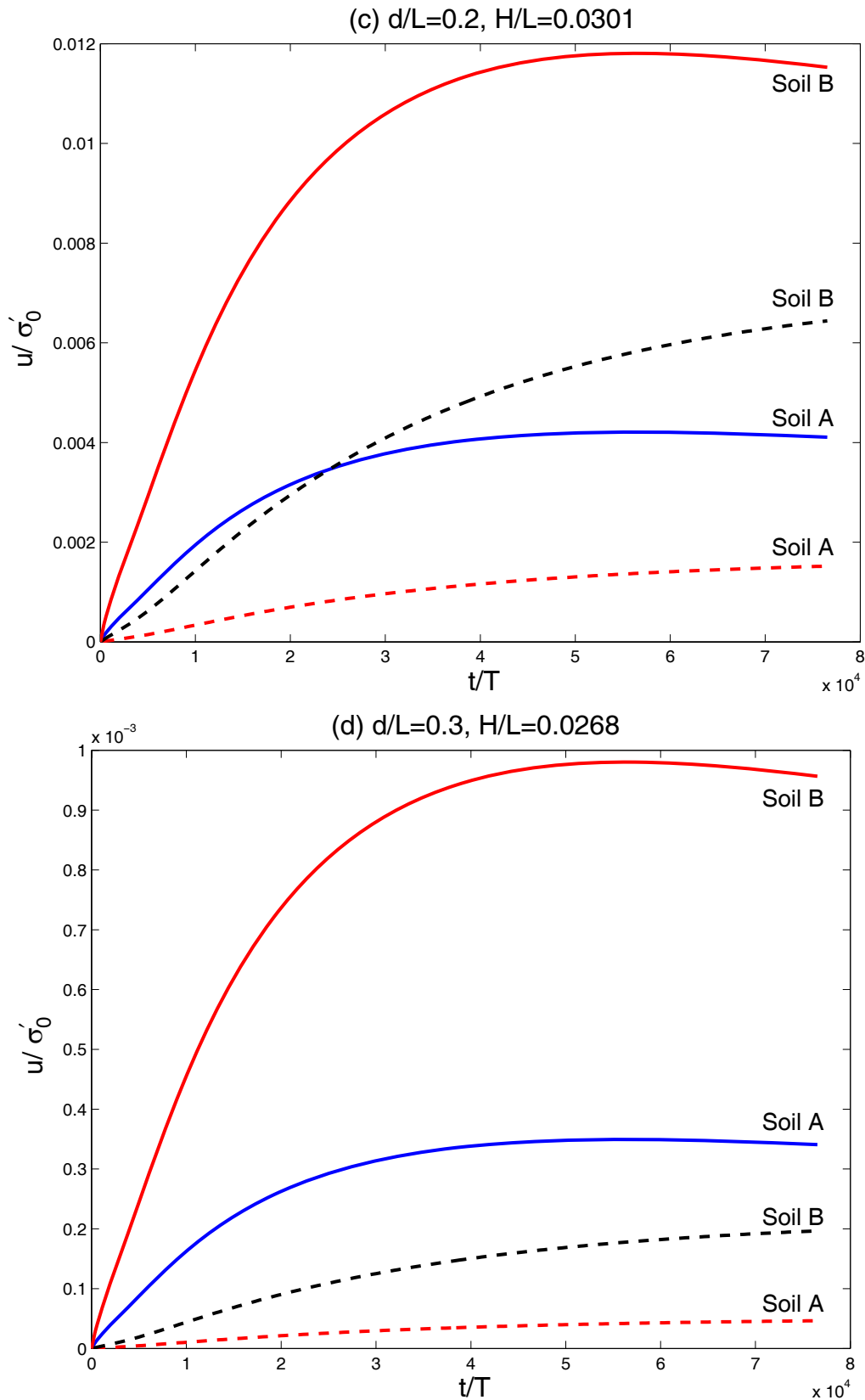


Figure 5(c)-(d): Time development of the pore pressure at $z=2\text{m}$, (---) linear relation, (—) non-linear relation. ($T=10$ sec, $h=20$ m). (c) $d/L=0.2, H/L=0.0301$; (d) $d/L=0.3, H/L=0.0268$.

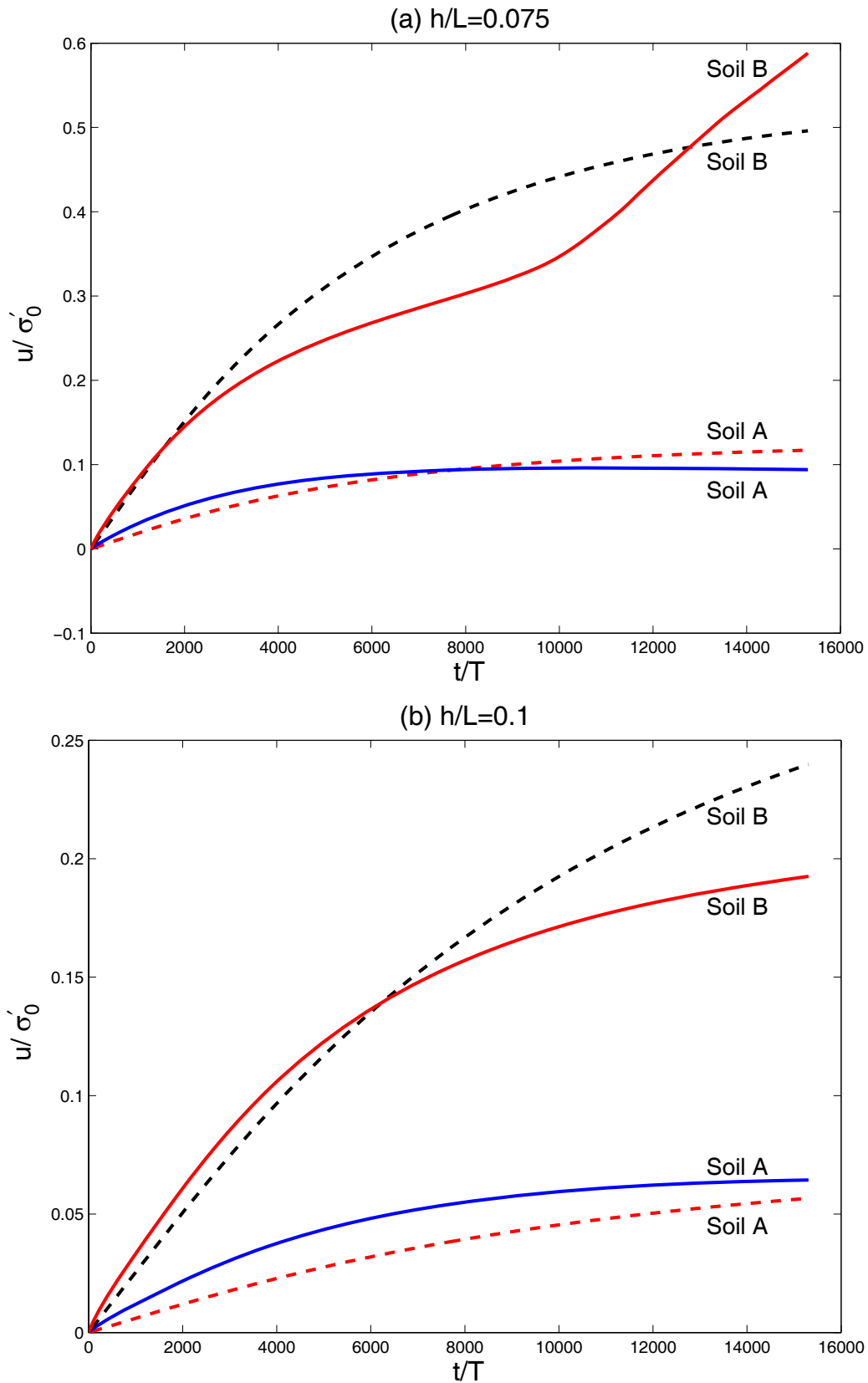


Figure 6(a)-(b): Time development of the pore pressure at $z=0.5587\text{m}$, (---) linear relation, (—) non-linear relation. ($T=10$ sec, $H=4$ m, $d=16$ m). (a) $h/L=0.075$, (b) $h/L=0.1$.

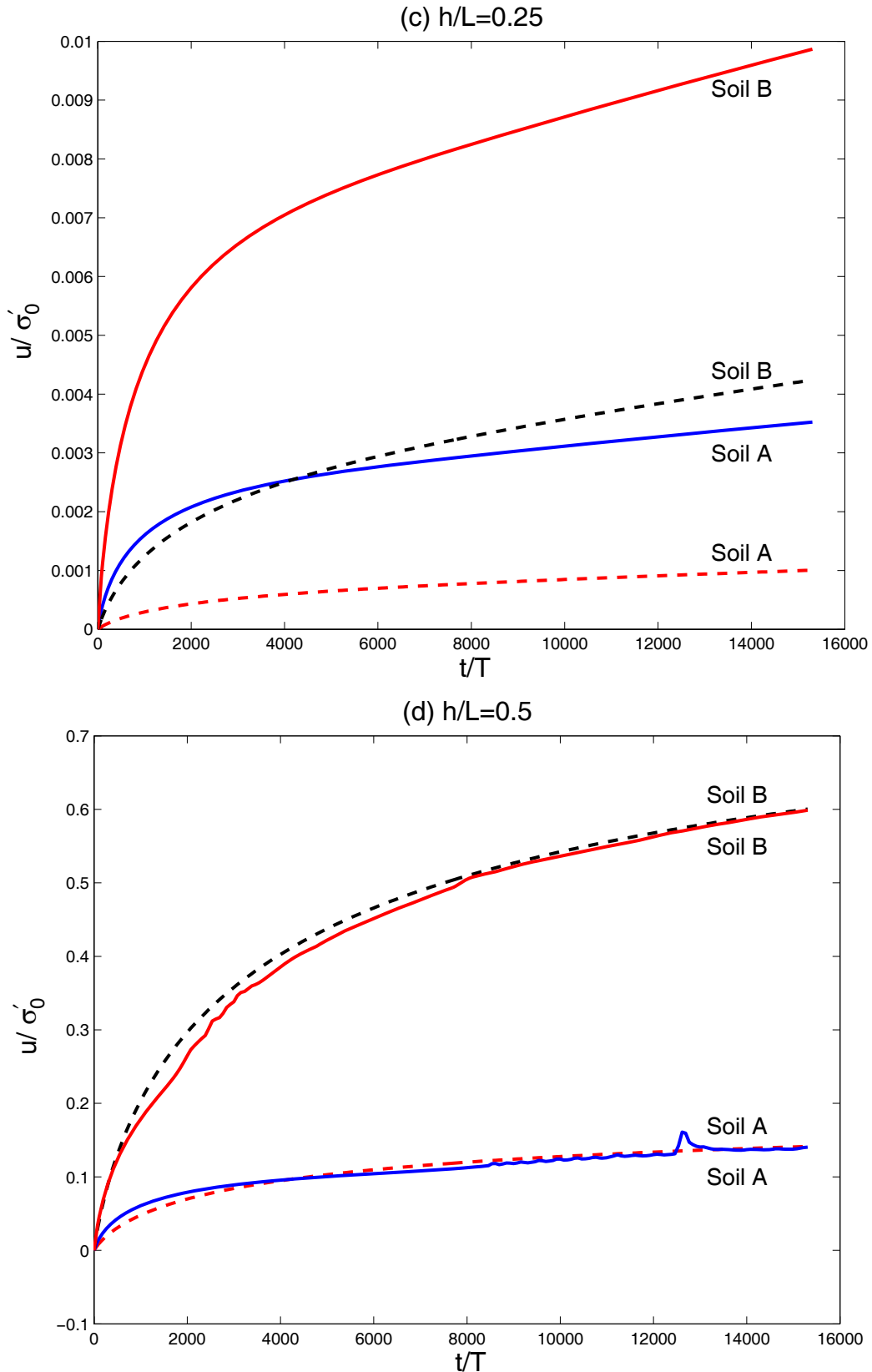


Figure 6 (c)-(d): Time development of the pore pressure at $z=0.5587\text{m}$, (---) linear relation, (—) non-linear relation. ($T=10$ sec, $H=4$ m, $d=16$ m). (c) $h/L=0.25$; (d) $h/L=0.5$.

6. A Simplified Approximation for an Infinite Seabed

6.1 Scaling analysis

The first objective of this study is to clarify the applicable ranges of the two mechanisms, We compare the amplitude of the oscillatory pore pressure ($|\tilde{p}|$) and the equilibrium residual pore pressure ($u(z, \infty)$):

$$P_{osc} = |\tilde{p}| = P_b \exp(-kz), \quad (35)$$

$$P_{res} = u(z, \infty) = \frac{2A}{c_v \lambda^3} \left[1 - \left(\frac{\lambda z}{2} + 1 \right) \exp(-\lambda z) \right]. \quad (36)$$

To examine the role of each mechanism, we define the amplitude ratio as

$$\varepsilon(z) = \frac{P_{res}}{P_{osc}}. \quad (37)$$

Distributions of the scaling factor (ε) versus soil depth (z/L) for various wave conditions are illustrated in Figure 7. Three different wave steepness and four relative water depths are considered. Figure 7 clearly indicates that the residual mechanism becomes more important as the scaling factor (ε) increases, the wave steepness (H/L) increases, or the relative water depth (d/L) decreases.

To further clarify the range of residual mechanism, we plot the critical line of $\varepsilon = 1$ with wave steepness and relative water depth at $z = 5$ m in Figure 8. The lines represent the critical relationship of H/L and d/L with given a consolidation coefficient (c_v). The region below the curve denotes conditions when the transient (oscillating) mechanism dominates, while the region above the curve denotes conditions when the residual mechanism dominates. The critical curve will move up as the consolidation coefficient (c_v) increases.

6.2 A simplified approximation for engineering practice

For engineers, the most important task is to examine where liquefaction will occur and how deep it is. The criterion of residual liquefaction is

$$\frac{P_{res}}{\sigma'_0} = 1, \quad (38)$$

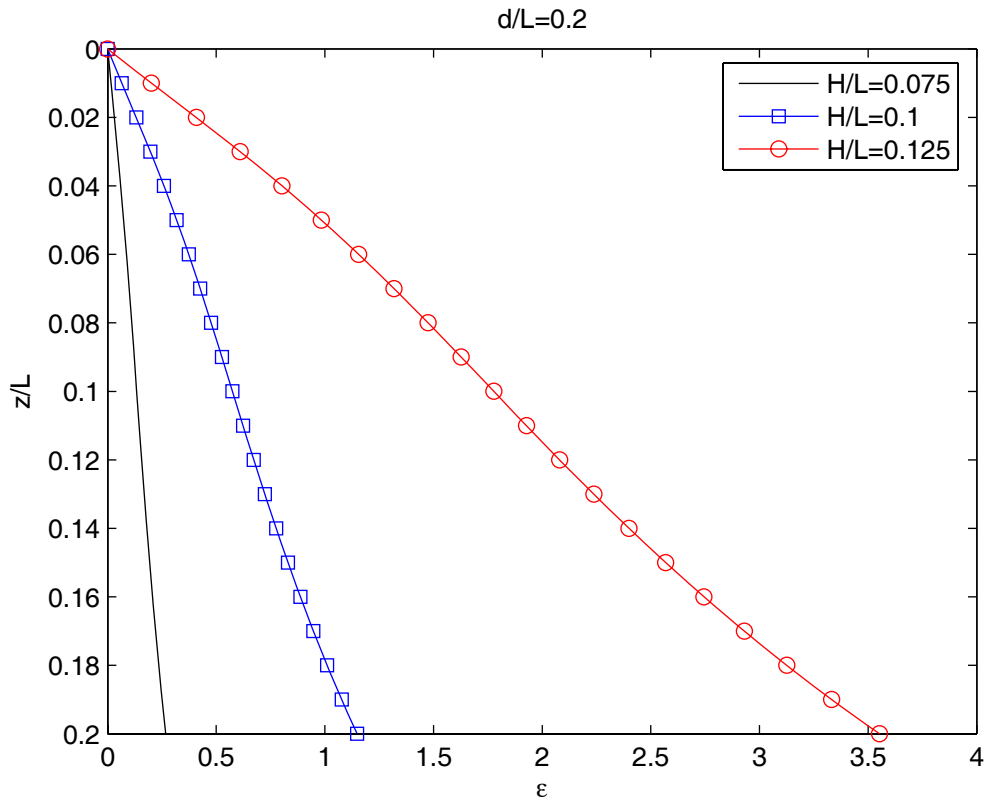
which leads to

$$\bar{p}(z, \infty) = \frac{2A}{c_v \lambda^3} \left[1 - \left(\frac{\lambda z_L}{2} + 1 \right) \exp(-\lambda z_L) \right] = \sigma'_0 = \frac{(1 + 2K_o)}{3} \gamma' z_L. \quad (39)$$

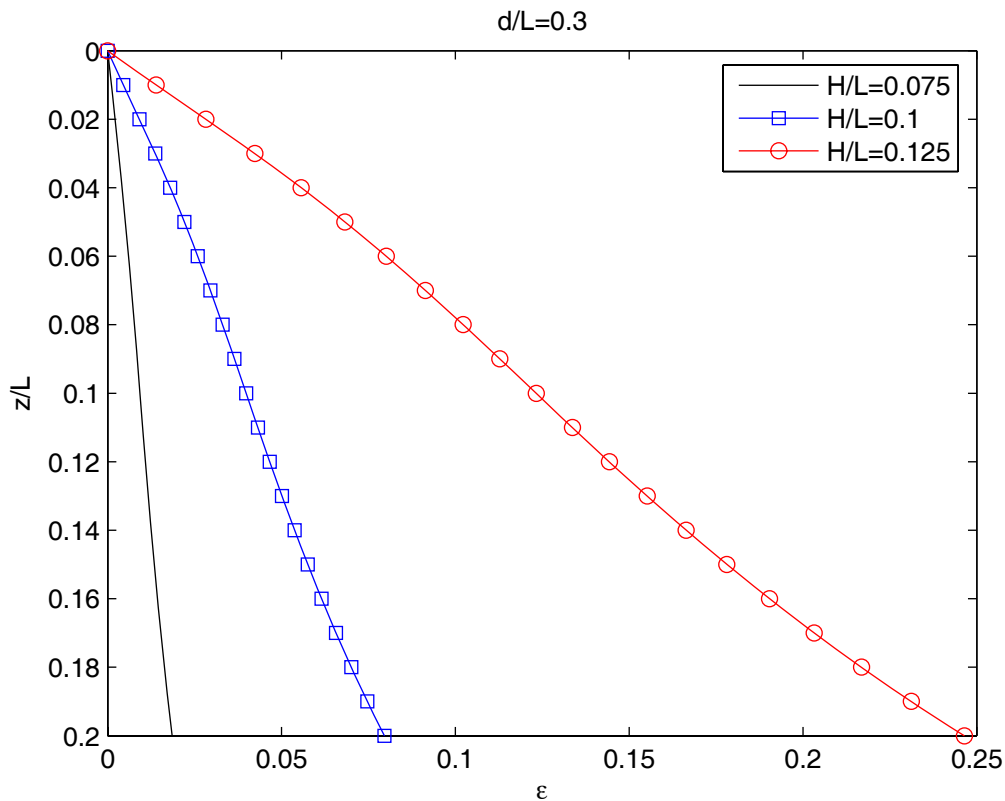
Let

$$B = \frac{(1 + 2K_o) \gamma' c_v \lambda^2}{6A}, \quad (40)$$

then Figure 9 shows the relationship of the maximum liquefied depth (z_L) and the parameter B . For engineering applications, given wave and soil conditions, we can determine the parameter B from (40). The maximum liquefied depth can then be easily determined from Figure 9. It is noted that the relation presented in Figure 9 is universal, applicable to all engineering conditions.



(a)



(b)

Figure 7 Distribution of the maximum scaling factor (ϵ) versus soil depth (z/L) for various wave steepness (H/L). (a) $d/L = 0.2$ and (b) $d/L = 0.3$. (Input data: $n_e=0.33$, $\mu=0.33$, $\alpha=0.246$, $c_v = 0.022$, $\eta=0.25$, and $T=10$ sec)

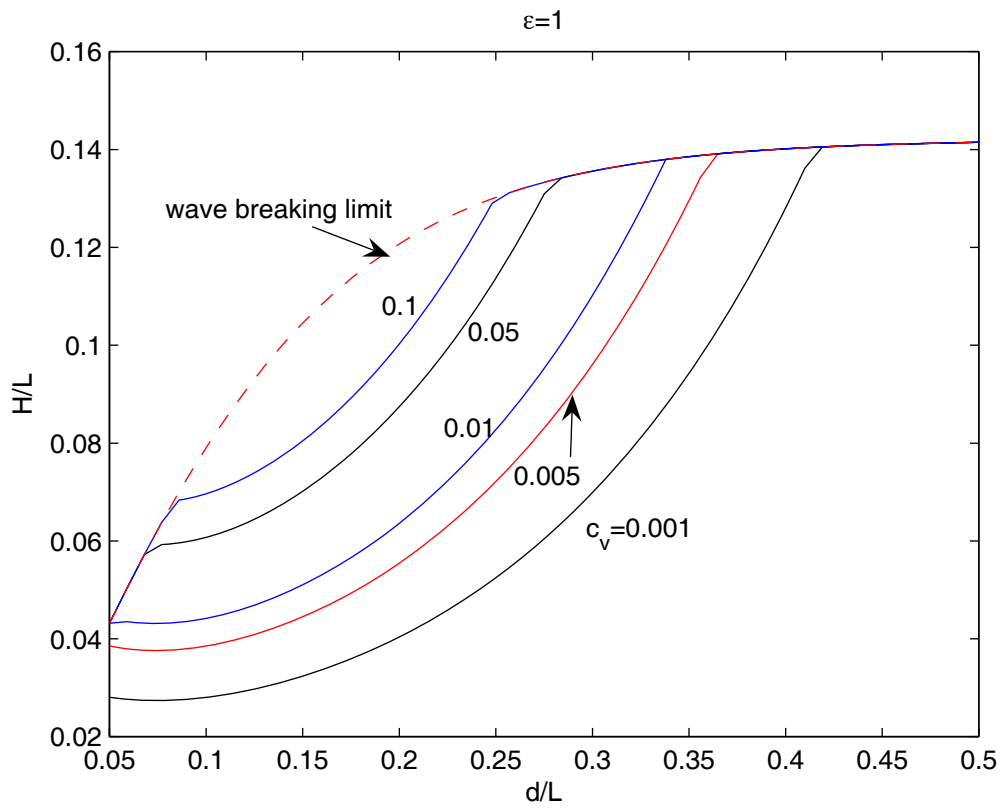


Figure 8 Distribution of critical wave steepness (H/L) versus relative water depth (d/L) for various value of consolidation coefficient (c_v) with $\varepsilon = 1$. (Input data: $n_e=0.33$, $\mu=0.33$, $\alpha=0.246$, $\eta=0.25$, and $T=10$ sec)

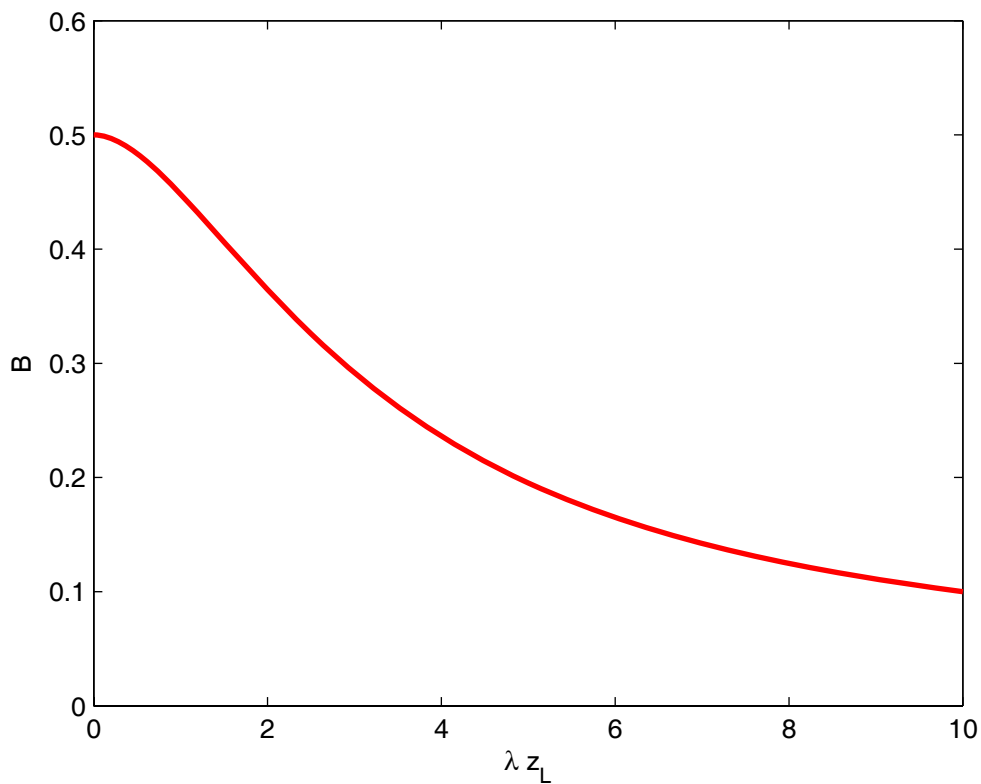


Figure 9 Distribution of the maximum liquefied depth (z_L) and parameter B .

7. Conclusions

In this study, the pore water pressure accumulation in marine sediments due to ocean waves is investigated. First, an analytical approximation is proposed for the linear relation of pore pressure generation. Then, a numerical scheme is employed for the case of a nonlinear relation. Based on the numerical results presented, the following conclusions can be drawn:

1. A comprehensive comparison between the present analytical approximation and numerical model against the experimental data (Clukey, *et al.*, 1983) was performed. The comparison indicates that the present models provide a better prediction of pore pressure accumulation than the previous analytical solution (McDougal, *et al.*, 1989).
2. An investigation of the effects of wave characteristics on the pore pressure accumulation was presented in Figures 2-5. The results indicate that the mechanism of pore pressure build-up and the nonlinear relation of pore pressure generation are more important under the conditions of (1) larger wave, (2) longer wave period, and (3) shallow water.
3. For soil characteristics, the pore pressure accumulates faster in shallow water and Soil A with a low consolidation coefficient.
4. A simplified approximation is proposed for the case of infinite seabed. Numerical results indicate that the residual mechanism is particularly important for large wave loading, while the oscillatory mechanism dominates the pore pressure under small wave loading. Figure 8 clearly indicates the range of residual mechanisms for various values of c_v .
5. Based on the new solution, a simplified approximation for the prediction of the maximum liquefaction depth is proposed for engineering practice. The universal relationship of the parameter B and the maximum liquefied depth (z_L) provides coastal geotechnical engineers a first-hand effective method for the evaluation of the residual liquefaction potential.

Acknowledgements

The authors are grateful for the support of Australian Research Council (ARC) Linkage-International Award #LX0455606 (2004-2007), USyd Research & Development Grant (2005) and USyd Bridge Research Grant (2006).

Appendix: Mathematical Derivations Of Analytical Solutions

A: Finite soil model

The boundary value problem for a seabed of finite depth are outlined here:

$$\frac{\partial u}{\partial t} = c_v \frac{\partial^2 u}{\partial z^2} + f, \quad (41)$$

$$u(z,0) = u(0,t) = 0, \quad (42)$$

$$\frac{\partial u(h,t)}{\partial z} = 0. \quad (43)$$

Since the source term is a time-independent function, the residual pore pressure (u) can be rewritten as

$$u = u_1(z) + u_2(z, t). \quad (44)$$

Then, the boundary value problem can be rewritten as

$$c_v \frac{\partial^2 u_1}{\partial z^2} = -f, \quad \frac{\partial u_2}{\partial t} = c_v \frac{\partial^2 u_2}{\partial z^2}, \quad (45)$$

$$u_1(0) = 0, \quad \frac{\partial u_1(h, t)}{\partial z} = 0, \quad (46)$$

$$u_2(z, 0) = 0, \quad u_2(0, t) = -u_1(0), \quad \frac{\partial u_2(h, t)}{\partial z} = 0, \quad (47)$$

The solution of $u_1(z)$ can be obtained through a Fourier series expansion and written as

$$u_1 = \sum_{n=1}^{\infty} a_n \sin\left(\frac{\kappa_n z}{h}\right), \quad a_n = \frac{2h}{c_v \kappa_n^2} \int_0^h f(r) \sin\left(\frac{\kappa_n r}{h}\right) dr, \quad (48)$$

Then, we can have the solution of $u_2(z, t)$ as

$$u_2 = -\sum_{n=1}^{\infty} e^{-c_v \kappa_n^2 t / h^2} a_n \sin\left(\frac{\kappa_n z}{h}\right) \quad (49)$$

The final solution of pore pressure will be identical to (21).

B. Shallow soil model

The solution for shallow soil model can be obtained with a similar framework as finite soil model. Thus, we can directly integrate (25) to obtain $u_1(z)$ as

$$u_1 = \frac{a}{2c_v} \left(h^2 z - \frac{z^3}{3} \right). \quad (50)$$

Again, we can have u_2 through a Fourier series expansion as

$$u_2 = -\frac{a}{2c_v} \sum_{n=1}^{\infty} a_n e^{-c_v \kappa_n^2 t / h^2} \sin\left(\frac{\kappa_n z}{h}\right), \quad a_n = \frac{2}{h} \int_0^h \left(h^2 r - \frac{r^3}{3} \right) \sin\left(\frac{\kappa_n r}{h}\right) dr. \quad (51)$$

Then, we have the solution for shallow soil model as (27).

C. Deep soil model

The boundary value problem for residual pore pressure in an infinite (deep) seabed can be summarized as:

$$\frac{\partial u}{\partial t} = c_v \frac{\partial^2 u}{\partial z^2} + A z e^{-\lambda z}, \quad (52)$$

$$u(0, t) = u(z, 0) = 0, \quad \text{and} \quad u(\infty, t) = 0. \quad (53)$$

Since it is an infinite domain, this can be easily solved by a Laplace transformation.

Now, we scale the problem as follows:

$$\zeta = c_v \lambda^2 t, \quad U = \frac{c_v \lambda^3 u}{A} \quad \text{and} \quad y = \lambda z. \quad (54)$$

Then, (52) and (53) become

$$U_\zeta = U_{yy} + ye^{-y} \quad \text{and} \quad U(0, \zeta) = U(y, 0) = 0. \quad (55)$$

Take Laplace transformation in ζ :

$$L(U(\zeta, y)) = Q(s, y) = \int_0^\infty e^{-s\zeta} U(\zeta, y) d\zeta. \quad (56)$$

Then

$$sQ = Q_{yy} + \frac{1}{s} ye^{-y} \quad \text{and} \quad Q(s, y) = 0, \quad Q(s, \infty) = 0. \quad (57)$$

The solution of (57) is

$$Q(s, y) = \frac{(ys - y - 2)}{s(s-1)^2} e^{-y} + \frac{2}{s(s-1)^2} e^{-\sqrt{s}y}. \quad (58)$$

We need to invert (58). Let's split into two parts:

$$R(s, y) = \frac{(ys - y - 2)}{s(s-1)^2} e^{-y} \quad \text{and} \quad V(s, y) = \frac{2}{s(s-1)^2} e^{-\sqrt{s}y}. \quad (59)$$

For $R(s, y)$ the inversion is straight forward: it has a simple pole at $s=0$ and a double pole at $s=1$. $V(s, y)$ has a branch point at $s=0$ and a double pole at $s=1$. This inversion entails a careful integration in the complex s -plane around a 'keyhole' contour. The combined inversion gives:

$$U(y, \zeta) = 2 \left[1 - \left(\frac{y}{2} + 1 \right) \right] e^{-y} - \frac{1}{\pi} \int_0^\infty \frac{e^{-r\zeta}}{r(r+1)^2} \sin(\sqrt{r}y) dr. \quad (60)$$

Now back in dimensional variables:

$$u = \frac{2A}{c_v \lambda^3} \left[1 - \left(\frac{\lambda z}{2} + 1 \right) \exp(-\lambda z) - \frac{1}{\pi} \int_0^\infty \frac{\exp(-rc_v \lambda^2 t)}{r(r+1)^2} \sin(\sqrt{r} \lambda z) dr \right], \quad (61)$$

which is identical to (31).

References

- Biot M.A., 1941. General theory of three-dimensional consolidation. *Journal of Applied Physics* 12,155-65.
- Cheng L., Sumer B.M., Fredsoe J., 2001. Solutions of pore pressure build up due to progressive waves. . *International Journal for Numerical and Analytical Methods in Geomechanics* 25,885-907.

- Clukey E.C., Kulhawy F.H., Liu P.L.-F. Laboratory and Field investigation of Wave-Sediment Interaction, Report 83-1. Joseph H. Defrees Hydraulics Laboratory, School of Civil and Environmental Engineering, Cornell University, Ithaca, N. Y 1983.
- De Alba P., Seed H.B., Chan C.K., 1976. Sand liquefaction in large-scale simple shear tests. *Journal of geotechnical Division, A. S. C. E.* 102,909-28.
- Hsu J.R.C., Jeng D.-S., 1994. Wave-induced soil response in an unsaturated anisotropic seabed of finite thickness. *International Journal for Numerical Analytical Methods in Geomechanics* 18(11),785-807.
- Jeng D.-S. Wave-Induced Seabed Response in Front of a Breakwater. Department of Environmental Engineering: The University of Western Australia, 1997. p. 297.
- Jeng D.-S., Hsu J.R.C., 1996. Wave-induced soil response in a nearly saturated seabed of finite thickness. *Geotechnique* 46(3),427-40.
- Jeng D.-S., Mao X., Enot P., Barry D.A., Li L., 41, , 2005. Spring-neap tide-induced beach water table fluctuations in a sloping coastal aquifer. *Water Resources Research* 41,doi:10.1029/2005WR003945.
- Kianoto T., Mase H., 1999. Boundary-Layer Theory for Anisotropic Seabed Response to Sea Waves. *Journal of Waterway, Port, Coastal and Ocean Engineering, A.S.C.E.* 125(4),187-94.
- Madsen O.S., 1978. Wave-induced pore pressure and effective stresses in a porous bed. *Geotechnique* 28,377-93.
- McDougal W.G., Tsai Y.T., Liu P.L.-F., Clukey E.C., 1989. Wave-induced pore water pressure accumulation in marine soils. *Journal of Offshore Mechanics and Arctic Engineering, A. S. M. E.* 111(1),1-11.
- Mei C.C., Foda M.A., 1981. Wave-induced response in a fluid-filled poroelastic solid with a free surface-A boundary layer theory. *Geophysical Journal of the Royal Astrological Society* 66,597-631.
- Miyamoto J., Sassa S., Sekiguchi H., 2004. Progressive solidification of a liquefied sand layer during continued wave loading. *Geotechnique* 54(10),617-29.
- Okusa S., 1985. Wave-induced stresses in unsaturated submarine sediments. *Geotechnique* 32(3),235-47.
- Sassa S., Sekiguchi H., 1999. Wave-induced liquefaction of beds of sand in centrifuge. *Geotechnique* 49(5),621-38.
- Sassa S., Sekiguchi H., 2001. Analysis of wave-induced liquefaction of sand beds. *Geotechnique* 51(12),115-26.
- Sassa S., Sekiguchi H., Miyamoto J., 2001. Analysis of progressive liquefaction as a moving-boundary problem. *Geotechnique* 51(10),847-57.
- Seed H.B., Rahman M.S., 1978. Wave-induced pore pressure in relation to ocean floor stability of cohesionless soil. *Marine Geotechnology* 3(2),123-50.
- Seed H.B., Martin P.O., Lysmer J. The Generation and Dissipation of Pore Water Pressure During Soil Liquefaction, Report EERC 75-26. College of Engineering, University of California, Berkeley, California 1975.
- Sekiguchi H., Kita K., Okamoto O., 1995. Response of poro-elastoplastic beds to standing waves. *Soils and Foundations* 35(3),31-42.
- Sumer B.M., Fredsoe J. The Mechanics of Scour in the Marine Environment World Scientific,, 2002 (536 pp.).

- Yamamoto T., Koning H., Sellmeijer H., Van Hijum E., 1978. On the response of a poroelastic bed to water waves. *Journal of Fluid Mechanics* 87,193-206.
- Yuhi M., Ishida H., 2002. Simplified solution of wave-induced seabed response in anisotropic seabed. *Journal of Waterway, Port, Coastal and Ocean Engineering*, A. S. C. E. 128(1),46-50.